



HHS Public Access

Author manuscript

ChemMedChem. Author manuscript; available in PMC 2024 March 27.

Published in final edited form as:

ChemMedChem. 2024 March 15; 19(6): e202300593. doi:10.1002/cmdc.202300593.

Synthesis and *in vitro* metabolic stability of sterically shielded antimycobacterial phenylalanine amides

Markus Lang^[a], Uday S. Ganapathy^[b], Lea Mann^[a], Rüdiger W. Seidel^[a], Richard Goddard^[c], Frank Erdmann^[a], Thomas Dick^{[b],[d],[e]}, Adrian Richter^[a]

^[a]Institut für Pharmazie, Martin-Luther-Universität Halle-Wittenberg, Wolfgang-Langenbeck-Str. 4, 06120 Halle (Saale), Germany

^[b]Center for Discovery and Innovation, Hackensack Meridian Health, 111 Ideation Way, 07110 Nutley, New Jersey, USA

^[c]Max-Planck-Institut für Kohlenforschung, Kaiser-Wilhelm-Platz 1, 45470 Mülheim an der Ruhr, Germany

^[d]Department of Medical Sciences, Hackensack Meridian School of Medicine, 123 Metro Blvd, 07110 Nutley, New Jersey, USA

^[e]Department of Microbiology and Immunology, Georgetown University, 3900 Reservoir Road, N.W., 20007 Washington DC, USA

Abstract

*N*α-aryyl-*N*-aryl-phenylalanine amides (AAPs) are RNA polymerase inhibitors with activity against *Mycobacterium tuberculosis* and non-tuberculous mycobacteria. We observed that AAPs rapidly degrade in microsomal suspensions, suggesting that avoiding hepatic metabolism is critical for their effectiveness *in vivo*. As both amide bonds are potential metabolic weak points of the molecule, we synthesized 16 AAP analogs in which the amide bonds are shielded by methyl or fluoro substituents in close proximity. Some derivatives show improved microsomal stability, while being plasma-stable and non-cytotoxic. In parallel with the metabolic stability studies, the antimycobacterial activity of the AAPs against *Mycobacterium tuberculosis*, *Mycobacterium abscessus*, *Mycobacterium avium* and *Mycobacterium intracellulare* was determined. The stability data are discussed in relation to the antimycobacterial activity of the panel of compounds and reveal that the concept of steric shielding of the anilide groups by a fluoro substituent has the potential to improve the stability and bioavailability of AAPs.

Graphical Abstract

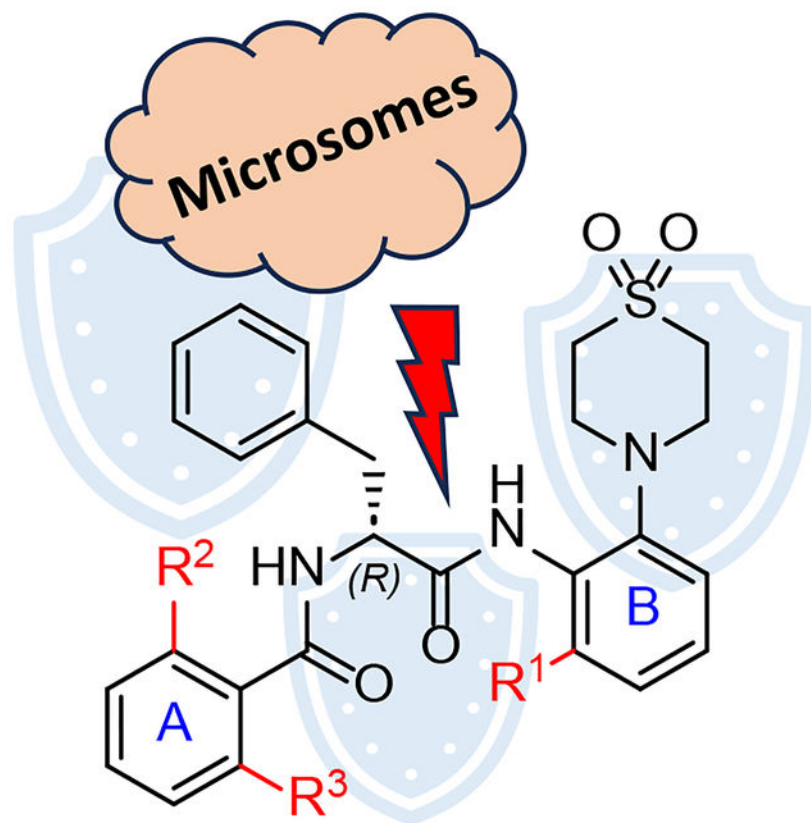
adrian.richter@pharmazie.uni-halle.de .

Supporting information for this article is given via a link at the end of the document.

Supporting Information

CCDC 2293688 contains the supplementary crystallographic data for this paper. These data can be obtained free of charge from the Cambridge Crystallographic Data Centre via www.ccdc.cam.ac.uk/structures.

The authors have cited additional references within the Supporting Information. [18, 30, 31, 35–47]



$N\alpha$ -aroyl- N -aryl-phenylalanine amides (AAPs) are active against numerous mycobacteria including *Mycobacterium tuberculosis* and *Mycobacterium abscessus*. As peptides, they are rapidly degraded in human and murine microsomal suspensions. Adding small substituents to the residues adjacent to the amide bonds, in particular at the anilide bond, results in increased stability.

Keywords

Phenylalanine amides; AAPs; *Mycobacterium abscessus*; microsomal stability; RNA polymerase

Introduction

Mycobacterium tuberculosis infections remain a significant global health concern¹, posing challenges to healthcare systems worldwide due to their persistence, potential for drug resistance, and the burden they impose on resources for diagnosis, treatment, and prevention²⁻⁵. Another growing healthcare concern are non-tuberculous mycobacteria (NTM)⁶, such as *Mycobacterium abscessus* (*Mabs*), that can cause severe infections of various organs, foremost in the respiratory tract⁷ that often require different treatment approaches in comparison to tuberculosis⁸⁻¹¹. Patients with underlying lung conditions, such as chronic obstructive pulmonary disease (COPD), cystic fibrosis (CF)¹², or a compromised immune system are particularly susceptible to NTM infections¹³. As the bacteria are commonly found in the environment, NTM are usually acquired from soil and water

sources. Patient-to-patient transmission can occur, and this particularly prominent among CF patients^{14,15}. Especially when *Mabs* is the causative agent, eradication of NTM infections is difficult owing to its inherent resistance to common antimycobacterial drugs^{16–18}. For this reason, new antimycobacterial agents are urgently needed.

MMV688845 (hereafter **MMV**) was first described as a hit structure against *Mycobacterium tuberculosis* (*Mtb*) and provides a potential chemical scaffold for further modification¹⁹. Ebright *et al* tested MMV anti-NTM properties and displayed *in vitro* activity against *Mycobacterium avium* (*Mavium*)²⁰. Screening the Pathogen Box (Medicines for Malaria Venture, Geneva, Switzerland) against *Mabs* and *Mavium*^{21–23} also identified **MMV** (Scheme 1A) as a promising hit compound against NTM^{21–23}. The closely related analogs D-AAP1 and D-IX336 were reported to inhibit mycobacterial RNA polymerase (RNAP) by targeting its β and β' subunits²⁴, thus inhibiting transcription. The *in vitro* generation and genome sequencing of **MMV** resistant mutants of *Mabs Bamboo* suggested that the same holds true for the hit compound²⁵. Rifamycins such as rifampicin, rifabutin and rifapentine are RNAP inhibitors that are currently in clinical use against many mycobacterial infections. Since *Mabs* exhibits intrinsic resistance mechanisms to rifampicin through C23 ribosylation^{26–28} and naphthohydroquinone oxidation²⁹, a therapy regimen that includes rifamycins is usually not an option. Consequently, there is a need to develop alternative RNAP inhibitors for anti-*Mabs* therapy. Cross-resistance of AAPs with rifamycins is unlikely as the target binding site of AAPs has been shown to be different²⁴, which has also been proven by *in vitro* experiments²⁵. Furthermore, the hit compound **MMV** was active against a variety of *Mabs* clinical isolates and exhibits bactericidal activity against *Mabs* in broth and in a macrophage infection model.¹⁰ AAPs are also of interest for the treatment of rifamycin-resistant *Mtb*, since they retain the effective bactericidal mechanism of RNAP inhibition while being chemically distinct.

Recently, we prepared analogs of **MMV** and obtained compounds with higher antimycobacterial activity, solubility, and plasma stability than the hit compound³⁰. We have established a synthetic pathway that retains the *R* configuration, which is necessary for the desired antimycobacterial activity, with *ee* values of 99%^{30,31}. In particular, the introduction of thiomorpholine dioxide instead of morpholine increased the whole cell activity. Compound **2** (Scheme 1B) displays an MIC₉₀ < 1 μ M against *Mabs* and *Mtb*.

Previous investigations on AAPs revealed that **MMV** gave insufficient plasma levels after oral administration in male Sprague Dawley rats^{23,32}. We have already presented plasma and microsomal stability data of the hit compound **MMV** and the highly active compound **24** (in this report called **2**) and revealed that **MMV** degraded quickly in murine plasma, whereas **2** was stable in both murine and human plasma³⁰. Amide moieties of drug candidates are known to be hydrolyzed in blood plasma to form inactive metabolites³³. The blood plasma of rodents typically exhibits higher and less specific hydrolase activity than human plasma due to differences in plasma esterases and their expression levels³⁴.

Both **MMV** and **2** were highly unstable during incubation with human and murine liver microsomes³⁰. AAPs contain two amide bonds which can undergo enzyme-catalyzed hydrolytic cleavage. The anilide is potentially more susceptible, since C-N π -bond overlap

of the amide group is weakened by the conjugation of the nitrogen atom with the phenyl group. Serine esterases such as carboxylesterases, which are predominantly found in the liver, are known to catalyze amide cleavage in humans³⁵. Another study also presents evidence for anilide cleavage in liver microsomes resulting in formation of an inactive drug candidate metabolite³⁶.

To address the poor hepatic stability of these compounds, we designed and synthesized a new series of AAP derivatives and performed *in vitro* characterization of plasma and microsomal stability, microbiological activity assessment against a variety of mycobacteria, cytotoxicity testing as well as solubility screening of the new substances.

Results and Discussion

Derivatization plan for increased metabolic stability

The derivatization strategy is based on analog **2** (Scheme 1B) that we developed, which shows increased *in vitro* activity against *Mabs* (MIC₉₀ = 0.78 μM)³⁰ compared to the initial hit **MMV** (MIC₉₀ = 6.25 μM). To gain structural insight, we subjected **2** to X-ray crystallography (Figure 1). In the crystal, **2** adopts the same conformation with an intramolecular N–H···O hydrogen bond similar to the previously described 2-thiophenoyl analog **MMV**³⁰. Likewise, the molecules form *pseudo* centrosymmetric N–H···O hydrogen bond dimers in the solid-state. Owing to the steric demand of the fluorine atom in the *ortho* position, the 2-fluorobenzene moieties are significantly tilted out of the plane of the attached amide groups. The 1,1-dioxo-1λ⁶-thiomorpholin-4-yl moiety appears to be primarily responsible for its increased potency and was therefore retained in the new AAPs.

We systematically derivatized various positions of the scaffold in the proximity of the amide bonds with the aim of sterically shielding the amide linkage and thereby prevent hydrolysis by amidases and esterases. This involved derivatization of positions 2 and 6, *ortho* positions to carbonyl, R² and R³, of aromatic system A as well as the *ortho* position of aromatic system B (R¹) adjacent to the anilide bond (Scheme 2A).

This approach was inspired by the development of lidocaine³⁹ in which methyl groups were introduced in order to prevent fast metabolism^{40–42}. Introduction of two methyl groups to procaine amide resulted in a conformational change (a twist of the benzene ring) sufficient to sterically shield the amide bond from hydrolysis by amidases⁴¹. Similar to this approach, the introduction of two *ortho* methyl groups in the aromatic system A could stabilize the amide towards metabolic hydrolysis. The peptides were also *N*-methylated to increase the stability (Scheme 2B). *N*-methylation can lead to higher serum stability of peptide like structures⁴³ and a higher stability against peptidases like chymotrypsin, as demonstrated by Haviv *et al.* in the synthesis of *N*-methyl leuprolide derivatives⁴⁴.

Results from Ebright *et al.* suggest that substituents that are bulkier than hydrogen, fluoro or methyl tend to result in lower antimycobacterial activities (e.g., *o*-chlorine ↓, 4-indolyl ↓, *o*-bromine ↓↓, *o*-ethyl ↓↓↓)²⁰. Thus, we restricted the study to small substituents, preferring fluorine and methyl to chlorine and bromine²⁰ to sterically shield the adjacent amide bond.

To the best of our knowledge, AAPs substituted in the *ortho* position to the anilide bond at aromatic system B (refer to Scheme 2A) have not been reported so far. In accordance with the approach employed in aromatic system A, we also elected to utilize less voluminous substituents to maximize the likelihood of achieving antimycobacterial activity. The addition of a methyl group is expected to result in a greater shielding effect due to its larger size compared to that of a fluorine atom.¹¹

Synthesis of 4-(2-aminophenyl)-1 λ ⁶-thiomorpholine-1,1-diones

The synthetic sequence commences with the synthesis of an aniline building block substituted with a thiomorpholine dioxide moiety in one *ortho*-position (Scheme 3). The other *ortho*-position is substituted with either hydrogen, fluorine atom, or a methyl group (as explained above).

In the initial step, various halogen-substituted nitrobenzenes were subject to aromatic nucleophilic substitutions. 1,3-Difluoro-2-nitrobenzene reacts smoothly with thiomorpholine dioxide owing to the strong electron deficiency caused by the two fluoro- and nitro substituents (Scheme 3A). The reaction of one equivalent of symmetric 1,3-difluoro-2-nitrobenzene with one equivalent of the nucleophile provides an efficient approach with a 95 % yield of the desired product. The mono-substituted product of the reaction did not undergo a second substitution reaction as it was less electrophilic than 1,3-difluoro-2-nitrobenzene.

Thiomorpholine dioxide is less nucleophilic than the corresponding thioether due to the electron-withdrawing effect of the sulfone group. Consequently, the unsubstituted³⁰ and 3-methyl nitrobenzene which are less electron-deficient than 1,3-difluoro-2-nitrobenzene had to be coupled with nucleophilic thiomorpholine and subsequently oxidized with *m*CPBA (Scheme 3B). Attempted reactions with thiomorpholine dioxide did not result in the desired product.

The *N*-methyl aniline moiety was obtained by initial formation of the formic acid amide of 2-morpholinoaniline and subsequent reduction to the secondary amine with LiAlH₄ (Scheme 3C)

Amide coupling with *N*-Boc-(*R*)-phenylalanine

To couple the previously synthesized anilines with *N*-Boc-(*R*)-phenylalanine or *N*-Boc-*N*-methyl-(*R*)-phenylalanine we utilized the coupling agent propane phosphonic acid anhydride (T3P)⁴⁵. In a former study T3P was found to be highly efficient for the synthesis of the AAP anilide structure while retaining the *R* configuration of the phenylalanine stereocenter^{30,46} which is essential for activity³¹. The reaction produced the desired 6-fluoro and 6-methyl derivatives at the R¹ position as well as the *N*-methylated derivatives (Scheme 4). A notable difference was observed in the yields of the reactions. The unsubstituted derivative yielded 99% product, while the 6-fluoro, 6-methyl and *N*-methyl derivatives gave yields of 92%, 56% and 33%, respectively. The particularly low yield of the 6-methyl and the *N*-methyl derivative indicate that the methyl groups sterically hinder the amine from attacking the electrophilic carbon atom.

Amide coupling with different benzoic acids

The final step of the synthetic sequence involves Boc-deprotection of the *N*-Boc-*(R)*-phenylalanine anilides (see Scheme 5) and the *N*-Boc-*N*-methyl-*(R)*-phenylalanine anilides (not shown) and subsequent amide coupling with a benzoic acid derivative. The Boc-deprotected intermediates were used for the amide coupling without further purification. For the formation of amides, 3-(diethoxyphosphoryloxy)-1,2,3-benzotriazin-4(3*H*)-one (DEPBT) and benzotriazol-1-yloxytripyrrolidinophosphonium hexafluorophosphate (PyBOP) were employed as effective and convenient coupling reagents for the synthesis of AAPs^{30,31} with retention of stereochemistry. PyBOP was used when conversion with DEPBT resulted in low yields. The conversion of 2,6-dimethylbenzoic acid proved challenging owing to the high degree of steric hindrance. In preliminary experiments, no consumption of the activated 2,6-dimethylbenzoic acid was observed when using DEPBT. Utilizing PyBOP as an alternative coupling reagent^{9,11} resulted in the formation of the desired products. Nevertheless, the yields remained relatively low at only 38% in two cases. All final products had >95 % purity, as determined by analytical HPLC.

In vitro plasma stability

All tested substances remained stable in human plasma over the test period of 120 min (as shown in Table 1). **MMV** exhibits a significant decrease in concentration in murine plasma³⁰. This result is comparable to the murine plasma stability published by Medicines for Malaria Venture (60% remaining substance after 4 h of incubation)³². The only other compound with a comparable fast degradation in murine plasma was **25**, which differs from **MMV** by only one *N*-methyl group (R⁵). In contrast, **29** did not show a similar drop in concentration, which is possibly due to the *N*-methyl group protecting the anilide (R⁴).

Our previous study showed a high human and murine plasma stability of **2**³⁰. We observed the same for the new derivatives described herein. Altering both the morpholine to thiomorpholine dioxide as well as the *N*α-2-thiophenoyl to *N*α-2-fluorobenzoyl and *N*α-2-methylbenzoyl groups appeared to sufficiently enhance the plasma stability of the compounds.

In vitro microsomal stability

All tested compounds showed a concentration decline in the microsomal suspensions (Table 2) used whereas stability in human microsomal suspensions was higher than in murine microsomal suspensions in every case analyzed (exemplary curves are depicted in Figure 2).

MMV showed particularly low stability in human and murine microsomal suspensions with only respectively 2 % and 0 % remaining after 7 min. These results of our study differ significantly from those published by Medicines for Malaria Ventures for **MMV**. While they reported half-lives of 129 minutes in human microsomal suspension and 795 minutes in murine microsomal suspension³². Our study found much lower half-lives of 1.2 and 0.9 minutes, respectively. The observed difference may be due to differences in assay conditions. Medicines for Malaria Venture report briefly on the assay conditions used, including a substrate concentration of 0.5 μM, 0.25 mg/mL microsomal proteins, and 50

mM phosphate buffer at pH 7.4³². In our assay, we used 2 μ M substrate concentration, 0.42 mg/mL microsomal proteins, and 100 mM phosphate buffer at pH 7.4. The authors did not disclose the usage of an NADPH-cofactor system, which is critical for oxidative metabolism catalyzed by microsomal enzymes. If this component is not utilized, it could explain the observed difference in microsomal stability.

The *N*-methylated compounds **25** and **29** did not exhibit superior performance to **MMV**. Compound **2**, the starting point for the series reported here, showed comparably low stabilities. This result shows that the sole replacement of morpholine by thiomorpholine dioxide and thiophene carboxylic acid amide by 2-fluoro benzoic acid amide does not increase the microsomal stability as was observed for the plasma stability.

Modifying the aromatic system A of **2** to provide further shielding of the adjacent amide bond only showed a slight tendency to increased microsomal stabilities, independent of which substituents were introduced. Increased stabilities were however achieved in combination with fluoro- and methyl-substitutions in aromatic system B. There was only a small increase in stability when 2-fluoro benzoic acid amide (aromatic system A) was used in combination with a fluoro-substituent at aromatic system B (compound **10**). Nevertheless, a tendency to higher stabilities could be observed with a methyl group in aromatic system B (compound **19**).

For all other substitution patterns in aromatic system A, increased stabilities were observed when combined with either methyl- or fluoro substitutions in aromatic system B. The highest stability increases in human microsomal suspensions (5.5- to 6.5-fold) were observed for **13** and **22** (a combination of *N* α -2-methylbenzoyl with 6-fluoro or 6-methyl substitutions, respectively). In contrast, the highest stability increases for murine microsomal suspensions (4- to 5-fold) were obtained with the combination of *N* α -2,6-difluorobenzoyl group together with 6-fluoro or 6-methyl substitutions.

Antimycobacterial activity assessment

Growth inhibition testing was performed through microdilution assays for a selection of mycobacteria. The results of the assays are depicted in Table 3.

The activities appear to be largely unaffected when aromatic system A was derivatized. Only the *N* α -2,6-dimethylbenzoyl derivative caused an overall decline in activity (see compounds **6** and **14**). All other substitution patterns are well accepted, with the tendency that the *N* α -2,6-difluorobenzoyl containing compounds showed the highest activities with **3** showing the highest activity (all activities in the nanomolar range). Even in combination with the fluoro-substituted aromatic system B, low micromolar activities against *Mavium* and *Mtb* and sub-micromolar activities against *Mycobacterium intracellulare* (*Mintra*) were observed (compound **11**). Particularly striking were the high activities of this compound class against the *Mintra* strain that we tested.

Changing the substitution pattern near and at the amide bonds strongly affected activity against the mycobacterial strains tested. The *N*-methylated compounds **25** and **29** suffered from complete activity loss, independent of the amide bond to which the *N*-methyl group

was added. Likewise, derivatization of aromatic system B caused strong declines in activity. The introduction of a fluoro substituent on the aromatic ring led to increased MIC₉₀ values, whereas the respective methyl substitution resulted in complete loss of activity. Only derivatives that contained a hydrogen atom next to the amide bond at aromatic system B showed improved MIC₉₀ values in comparison to the hit compound.

Cytotoxicity

The compounds synthesized in this study were tested for their single concentration cytotoxicity against an immortalized the human kidney epithelia cell line HEK293. To the best of our knowledge, AAPs have never been tested against this cell line. Cell viability relative to a DMSO-treated control is depicted in Figure 3.

Only three compounds caused a relative cell viability lower than 90 %, including the hit compound **MMV** (67 % viability) and also **2** (73 % viability), which demonstrated high antimycobacterial activities. Both compounds have been tested against a variety of cell lines and displayed no concerning behavior^{30–32}. The *N*-methyl compound **25** exhibited the highest cytotoxicity with only 35% viability. In contrast, the other *N*-methyl compound (**29**) did not demonstrate a high degree of cytotoxicity.

Conclusions

Microsomal stability as a model for hepatic stability was used as an indicator of intrinsic clearance for AAPs. We observed that sterically shielding the amide bonds within the molecular structures of AAPs increases their microsomal stability. In particular, shielding of the anilide bond at the aromatic system B resulted in higher stabilities in microsomal suspensions.

Methyl substituents result in complete loss of whole cell activity, rendering these molecules unsuitable for further efficacy development, although compounds within this group demonstrated improved stabilities against murine (**20**) and human (**22**) microsomes. Antimycobacterial activity was observed with fluoro substituents making the respective fluorinated AAPs valuable option for future efficacy development. The compound **11**, which carries fluorine atoms at all investigated positions, possess MIC₉₀ values between 0.4 and 12.5 μ M depending on the mycobacterial species combined with improved microsomal stabilities.

Modification of the aromatic system A was tolerated well with regard to the potency of the compounds. *N* α -2,6-dimethylbenzoyl and *N* α -2,6-difluorobenzoyl groups were found to be beneficial to microsomal stability, offering compounds that show higher or equal activities together with higher stabilities in comparison to both the hit compound and the most active compound **2** published so far.

N-methylation of the anilide bond resulted in increased plasma stability, whereas *N*-methylation of the *N* α -2-thiophenyl groups did not cause the same effect. This suggests that the anilide bond of the hit compound is susceptible to hydrolysis and that it is stabilized by an adjacent *N*-methyl group.

Based on these results, we conclude that the AAP derivatives investigated have sufficient plasma stability for activity even without *N*-methylation, which is an improvement compared to the hit compound **MMV**. Thus, cleavage or metabolization by plasma components probably does not contribute to low *in vivo* plasma levels to a relevant extent.

These findings support the view that the stability issues of AAPs are probably due to the instability of the amide bonds. Useful additional information is provided by the observation that shielding of the anilide bond in aromatic system **B** results in increased stability. Future studies on resulting metabolites will aid the design of AAPs for improved stability and activity.

Supplementary Material

Refer to Web version on PubMed Central for supplementary material.

Acknowledgements

We would like to thank Nadine Jänckel, Dr. Nadine Taudte and Dr. Jens-Ulrich Rahfeld for providing and maintaining the biosafety level 2 facility, and Dr. Christian Ihling and Antje Herbrich-Peters for measuring the HRMS spectra.

This work was funded by the Deutsche Forschungsgemeinschaft (DFG, German Research Foundation)—432291016, the National Institute of Allergy and Infectious Diseases of the National Institutes of Health under award number R01AI132374 and Mukoviszidose Institut gGmbH project number 2202 (Bonn, Germany), the research and development arm of the German Cystic Fibrosis Association Mukoviszidose e. V.

References

- (1). World Health Organization. Global Tuberculosis Report 2023. <https://www.who.int/teams/global-tuberculosis-programme/tb-reports/global-tuberculosis-report-2023> (accessed 2023-12-18).
- (2). Malenfant JH; Brewer TF Rifampicin Mono-Resistant Tuberculosis—A Review of an Uncommon But Growing Challenge for Global Tuberculosis Control. *Open Forum Infect Dis* 2021, 8 (2). 10.1093/OFID/OFAB018.
- (3). Shah I; Poojari V; Meshram H Multi-Drug Resistant and Extensively-Drug Resistant Tuberculosis. *Indian J Pediatr* 2020, 87 (10), 833–839. 10.1007/S12098-020-03230-1/TABLES/2. [PubMed: 32103425]
- (4). Seaworth BJ; Griffith DE Therapy of Multidrug-Resistant and Extensively Drug-Resistant Tuberculosis. *Microbiol Spectr* 2017, 5 (2). 10.1128/MICROBIOLSPEC.TNMI7-0042-2017.
- (5). Conradie F; Diacon AH; Ngubane N; Howell P; Everitt D; Crook AM; Mendel CM; Egizi E; Moreira J; Timm J; McHugh TD; Wills GH; Bateson A; Hunt R; Van Niekerk C; Li M; Olugbosi M; Spigelman M Treatment of Highly Drug-Resistant Pulmonary Tuberculosis. *New England Journal of Medicine* 2020, 382 (10), 893–902. 10.1056/NEJMOA1901814. [PubMed: 32130813]
- (6). Prevots DR; Marshall JE; Wagner D; Morimoto K Global Epidemiology of Nontuberculous Mycobacterial Pulmonary Disease: A Review. *Clin Chest Med* 2023. 10.1016/J.CCM.2023.08.012.
- (7). Johansen MD; Herrmann JL; Kremer L Non-Tuberculous Mycobacteria and the Rise of Mycobacterium Abscessus. *Nat Rev Microbiol* 2020, 18 (7), 392–407. 10.1038/S41579-020-0331-1. [PubMed: 32086501]
- (8). Yan M; Brode SK; Marras TK Treatment of the Less Common Nontuberculous Mycobacterial Pulmonary Disease. *Clin Chest Med* 2023. 10.1016/j.ccm.2023.06.011.
- (9). Daley CL; Iaccarino JM; Lange C; Cambau E; Wallace RJ; Andrejak C; Böttger EC; Brozek J; Griffith DE; Guglielmetti L; Huitt GA; Knight SL; Leitman P; Marras TK; Olivier KN; Santin M; Stout JE; Tortoli E; Van Ingen J; Wagner D; Winthrop KL Treatment of Nontuberculous

Mycobacterial Pulmonary Disease: An Official Ats/Ers/Escomid/Idsa Clinical Practice Guideline. *Clinical Infectious Diseases* 2020, 71 (4), E1–E36. 10.1093/CID/CIAA241. [PubMed: 32628747]

- (10). Nguyen M-VH; Daley CL Treatment of Mycobacterium Avium Complex Pulmonary Disease: When Should I Treat and What Therapy Should I Start? *Clin Chest Med* 2023. 10.1016/j.ccm.2023.06.009.
- (11). Holt MR; Baird T Treatment Approaches to Mycobacterium Abscessus Pulmonary Disease. *Clin Chest Med* 2023. 10.1016/j.ccm.2023.06.010.
- (12). Baird T; Bell S Cystic Fibrosis-Related Nontuberculous Mycobacterial Pulmonary Disease. *Clin Chest Med* 2023. 10.1016/j.ccm.2023.06.008.
- (13). Loebinger MR; Quint JK; van der Laan R; Obradovic M; Chawla R; Kishore A; van Ingen J Risk Factors for Nontuberculous Mycobacterial Pulmonary Disease: A Systematic Literature Review and Meta-Analysis. *Chest* 2023, 164 (5), 1115–1124. 10.1016/J.CHEST.2023.06.014. [PubMed: 37429481]
- (14). Ruis C; Bryant JM; Bell SC; Thomson R; Davidson RM; Hasan NA; van Ingen J; Strong M; Floto RA; Parkhill J Dissemination of Mycobacterium Abscessus via Global Transmission Networks. *Nature Microbiology* 2021 6:10 2021, 6 (10), 1279–1288. 10.1038/s41564-021-00963-3.
- (15). Aitken ML; Limaye A; Pottinger P; Whimbey E; Goss CH; Tonelli MR; Cangelosi GA; Ashworth Dirac M; Olivier KN; Brown-Elliott BA; McNulty S; Wallace RJ Respiratory Outbreak of Mycobacterium Abscessus Subspecies Massiliense in a Lung Transplant and Cystic Fibrosis Center. *Am J Respir Crit Care Med* 2012, 185 (2), 231–232. 10.1164/AJRCCM.185.2.231. [PubMed: 22246710]
- (16). Johnson MM; Odell JA Nontuberculous Mycobacterial Pulmonary Infections. *J Thorac Dis* 2014, 6 (3), 210. 10.3978/J.ISSN.2072-1439.2013.12.24. [PubMed: 24624285]
- (17). Lopeman RC; Harrison J; Desai M; Cox JAG Mycobacterium Abscessus: Environmental Bacterium Turned Clinical Nightmare. *Microorganisms* 2019, Vol. 7, Page 90 2019, 7 (3), 90. 10.3390/MICROORGANISMS7030090. [PubMed: 30909391]
- (18). Nessar R; Cambau E; Reytrat JM; Murray A; Gicquel B Mycobacterium Abscessus: A New Antibiotic Nightmare. *Journal of Antimicrobial Chemotherapy* 2012, 67 (4), 810–818. 10.1093/JAC/DKR578. [PubMed: 22290346]
- (19). Ballell L; Bates RH; Young RJ; Alvarez-Gomez D; Alvarez-Ruiz E; Barroso V; Blanco D; Crespo B; Escribano J; González R; Lozano S; Huss S; Santos-Villarejo A; Martín-Plaza JJ; Mendoza A; Rebollo-Lopez MJ; Remuñan-Blanco M; Lavandera JL; Pérez-Herran E; Gamo-Benito FJ; García-Bustos JF; Barros D; Castro JP; Cammack N Fueling Open-Source Drug Discovery: 177 Small-Molecule Leads against Tuberculosis. *ChemMedChem* 2013, 8 (2), 313–321. 10.1002/CMDC.201200428. [PubMed: 23307663]
- (20). Ebright Richard H.; Ebright Yon W.; Mandal Soma; Wilde Richard; Li S Preparation of N-Alpha-Aroyl-N-Aryl-Phenylalaninamides as Inhibitors of Bacterial RNA Polymerase and as Antibacterials. WO2015120320 A1 2015-08-13, 2015.
- (21). Richter A; Strauch A; Chao J; Ko M; Av-Gay Y Screening of Preselected Libraries Targeting Mycobacterium Abscessus for Drug Discovery. *Antimicrob Agents Chemother* 2018, 62 (9). 10.1128/AAC.00828-18.
- (22). Jeong J; Kim G; Moon C; Kim HJ; Kim TH; Jang J Pathogen Box Screening for Hit Identification against Mycobacterium Abscessus. *PLoS One* 2018, 13 (4), e0195595. 10.1371/JOURNAL.PONE.0195595. [PubMed: 29698397]
- (23). Low JL; Wu ML; Aziz DB; Laleu B; Dick T Screening of TB Actives for Activity against Nontuberculous Mycobacteria Delivers High Hit Rates. *Front Microbiol* 2017, 8 (AUG), 1539. 10.3389/FMICB.2017.01539. [PubMed: 28861054]
- (24). Lin W; Mandal S; Degen D; Liu Y; Ebright YW; Li S; Feng Y; Zhang Y; Mandal S; Jiang Y; Liu S; Gigliotti M; Talaue M; Connell N; Das K; Arnold E; Ebright RH Structural Basis of Mycobacterium Tuberculosis Transcription and Transcription Inhibition. *Mol Cell* 2017, 66 (2), 169–179.e8. 10.1016/j.molcel.2017.03.001. [PubMed: 28392175]

- (25). Mann L; Ganapathy US; Abdelaziz R; Lang M; Zimmerman MD; Dartois V; Dick T; Richter A In Vitro Profiling of the Synthetic RNA Polymerase Inhibitor MMV688845 against Mycobacterium Abscessus. *Microbiol Spectr* 2022, 10 (6). 10.1128/SPECTRUM.02760-22.
- (26). Rominski A; Roditscheff A; Selchow P; Böttger EC; Sander P Intrinsic Rifamycin Resistance of Mycobacterium Abscessus Is Mediated by ADP-Ribosyltransferase MAB_0591. *Journal of Antimicrobial Chemotherapy* 2017, 72 (2), 376–384. 10.1093/JAC/DKW466. [PubMed: 27999011]
- (27). Lan T; Ganapathy US; Sharma S; Ahn Y-M; Zimmerman M; Molodtsov V; Hegde P; Gengenbacher M; Ebright RH; Dartois V; Freundlich JS; Dick T; Aldrich CC Redesign of Rifamycin Antibiotics to Overcome ADP-Ribosylation-Mediated Resistance. *Angewandte Chemie* 2022, 134 (45), e202211498. 10.1002/ANGE.202211498.
- (28). Zaw MT; Emran NA; Lin Z Mutations inside Rifampicin-Resistance Determining Region of RpoB Gene Associated with Rifampicin-Resistance in Mycobacterium Tuberculosis. *J Infect Public Health* 2018, 11 (5), 605–610. 10.1016/J.JIPH.2018.04.005. [PubMed: 29706316]
- (29). Ganapathy US; Lan T; Krastel P; Lindman M; Zimmerman MD; Ho HP; Sarathy JP; Evans JC; Dartois V; Aldrich CC; Dick T Blocking Bacterial Naphthohydroquinone Oxidation and Adribosylation Improves Activity of Rifamycins against Mycobacterium Abscessus. *Antimicrob Agents Chemother* 2021, 65 (9). <https://doi.org/10.1128/AAC.00978-21>.
- (30). Lang M; Ganapathy US; Mann L; Abdelaziz R; Seidel RW; Goddard R; Sequenzia I; Hoenke S; Schulze P; Aragaw WW; Csuk R; Dick T; Richter A Synthesis and Characterization of Phenylalanine Amides Active against Mycobacterium Abscessus and Other Mycobacteria. *J Med Chem* 2023. 10.1021/ACS.JMEDCHEM.3C00009.
- (31). Mann L; Lang M; Schulze P; Halz JH; Csuk R; Hoenke S; Seidel RW; Richter A Racemization-Free Synthesis of N α -2-Thiophenoyl-Phenylalanine-2-Morpholinoanilide Enantiomers and Their Antimycobacterial Activity. *Amino Acids* 2021, 53 (8), 1187–1196. 10.1007/S00726-021-03044-1. [PubMed: 34259925]
- (32). Medicines for Malaria Venture. Biological Data and DMPK Data of the Pathogen Box Compounds. <https://www.mmv.org/mmv-open/pathogen-box/about-pathogen-box> (accessed 2024-01-31).
- (33). Beuchel A; Robaa D; Negatu DA; Madani A; Alvarez N; Zimmerman MD; Richter A; Mann L; Hoenke S; Csuk R; Dick T; Imming P Structure–Activity Relationship of Anti-Mycobacterium Abscessus Piperidine-4-Carboxamides, a New Class of NBTI DNA Gyrase Inhibitors. *ACS Med Chem Lett* 2022, acsmedchemlett.1c00549. 10.1021/ACSMEDCHEMLETT.1C00549.
- (34). Bahar FG; Ohura K; Ogihara T; Imai T Species Difference of Esterase Expression and Hydrolase Activity in Plasma. *J Pharm Sci* 2012, 101 (10), 3979–3988. 10.1002/JPS.23258. [PubMed: 22833171]
- (35). Bradshaw PR; Wilson ID; Gill RU; Butler PJ; Dilworth C; Athersuch TJ Metabolic Hydrolysis of Aromatic Amides in Selected Rat, Minipig, and Human In Vitro Systems. *Scientific Reports* 2018 8:1 2018, 8 (1), 1–8. 10.1038/s41598-018-20464-4. [PubMed: 29311619]
- (36). Liu L; Halladay JS; Shin Y; Wong S; Coraggio M; La H; Baumgardner M; Le H; Gopaul S; Boggs J; Kuebler P; Davis JC Jr; Charlene Liao X; Lubach JW; Deese A; Gregory Sowell C; Currie KS; Young WB; Cyrus Khojasteh S; C A Hop CE; Wong H Significant Species Difference in Amide Hydrolysis of GDC-0834, a Novel Potent and Selective Bruton’s Tyrosine Kinase Inhibitor. 2011. 10.1124/dmd.111.040840.
- (37). Midgley L; Bourhis LJ; Dolomanov OV; Grabowsky S; Kleemiss F; Puschmann H; Peyerimhoff N Vanishing of the Atomic Form Factor Derivatives in Non-Spherical Structural Refinement - a Key Approximation Scrutinized in the Case of Hirshfeld Atom Refinement. *Acta Crystallogr A Found Adv* 2021, 77 (6), 519–533. 10.1107/S2053273321009086. [PubMed: 34726630]
- (38). Kleemiss F; Dolomanov OV; Bodensteiner M; Peyerimhoff N; Midgley L; Bourhis LJ; Genoni A; Malaspina LA; Jayatilaka D; Spencer JL; White F; Grundkötter-Stock B; Steinhauer S; Lentz D; Puschmann H; Grabowsky S Accurate Crystal Structures and Chemical Properties from NoSpherA2. *Chem Sci* 2021, 12 (5), 1675–1692. 10.1039/D0SC05526C.
- (39). Ruetsch Y; Boni T; Borgeat A From Cocaine to Ropivacaine: The History of Local Anesthetic Drugs. *Curr Top Med Chem* 2001, 1 (3), 175–182. 10.2174/1568026013395335. [PubMed: 11895133]

- (40). Robert A; Schultz JR; Nezamis JE; Lancaster C Gastric Antisecretory and Antiulcer Properties of PGE₂, 15-Methyl PGE₂, and 16, 16-Dimethyl PGE₂. Intravenous, Oral and Intrajejunal Administration. *Gastroenterology* 1976, 70 (3), 359–370. 10.1016/S0016-5085(76)80147-3. [PubMed: 174967]
- (41). Barreiro EJ; Kümmerle AE; Fraga CAM The Methylation Effect in Medicinal Chemistry. *Chem Rev* 2011, 111 (9), 5215–5246. 10.1021/CR200060G. [PubMed: 21631125]
- (42). Dajani EZ; Driskill DR; Bianchi RG; Collins PW; Pappo R SC-29333: A Potent Inhibitor of Canine Gastric Secretion. *Am J Dig Dis* 1976, 21 (12), 1049–1057. 10.1007/BF01071862. [PubMed: 797257]
- (43). Van Neer RHP; Dranchak PK; Liu L; Aitha M; Queme B; Kimura H; Katoh T; Battaile KP; Lovell S; Inglese J; Suga H Serum-Stable and Selective Backbone-N-Methylated Cyclic Peptides That Inhibit Prokaryotic Glycolytic Mutases. *ACS Chem Biol* 2022, 17 (8), 2284–2295. 10.1021/ACSCHEMBIO.2C00403. [PubMed: 35904259]
- (44). Haviv F; Fitzpatrick TD; Swenson RE; Nichols CJ; Mort NA; Bush EN; Diaz G; Bammert G; Nguyen A; Rhutasel NS; Nellans HN; Hoffman DJ; Johnson ES; Greer J Effect of N-Methyl Substitution of the Peptide Bonds in Luteinizing Hormone-Releasing Hormone Agonists. *J Med Chem* 1993, 36 (3), 363–369. 10.1021/JM00055A007. [PubMed: 8381183]
- (45). García ALL T3P: A Convenient and Useful Reagent in Organic Synthesis. *Synlett* 2007, 2007 (08), 1328–1329. 10.1055/S-2007-980339.
- (46). Dunetz JR; Xiang Y; Baldwin A; Ringling J General and Scalable Amide Bond Formation with Epimerization-Prone Substrates Using T3P and Pyridine. *Org Lett* 2011, 13 (19), 5048–5051. 10.1021/OL201875Q. [PubMed: 21875100]

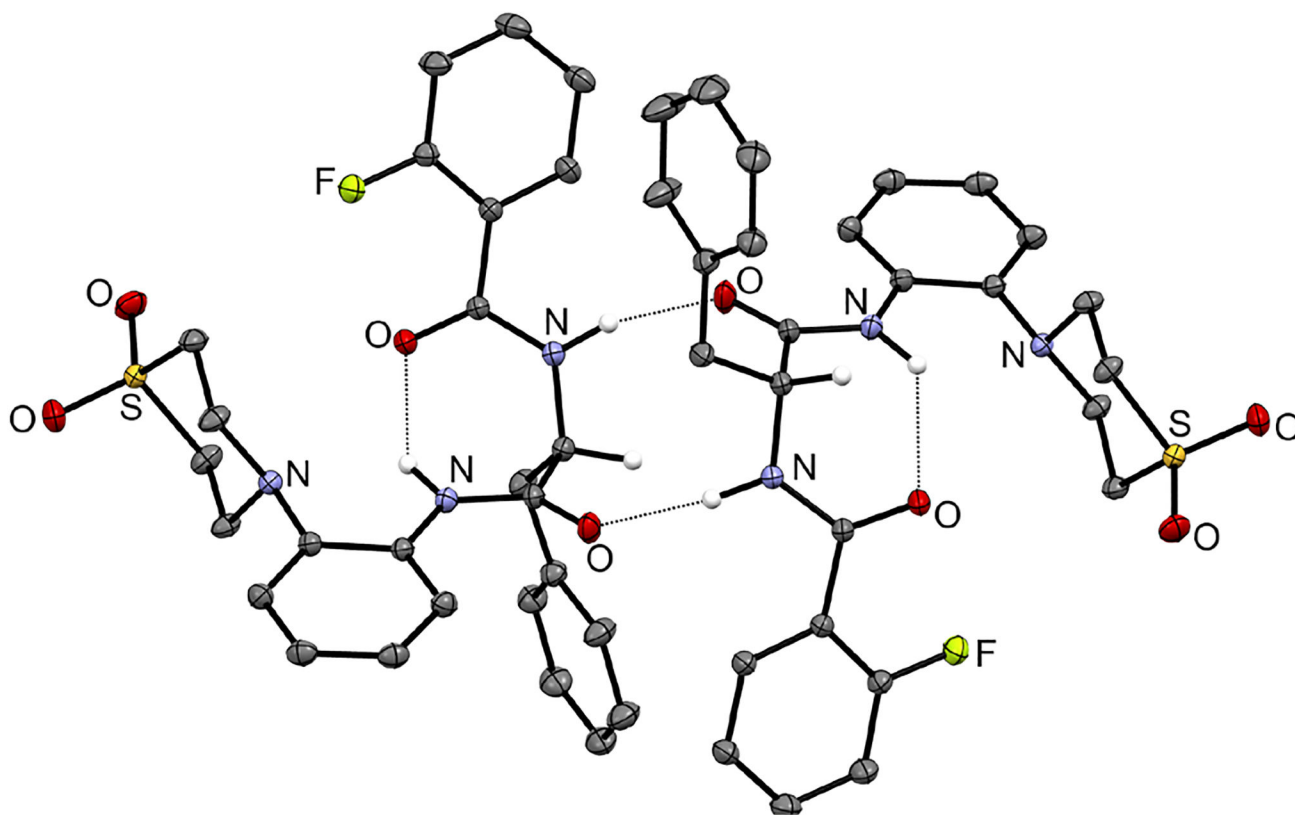


Figure 1.

Asymmetric unit of **2**. Displacement ellipsoids are drawn at the 50 % probability level. Nitrogen-bound hydrogen atoms and the carbon-bound hydrogen atoms attached to centers of chirality are represented by small spheres of arbitrary radius, otherwise hydrogen atoms are omitted for clarity. Dashed lines represent hydrogen bonds. Colour scheme: C, grey; H, white; N, blue; O, red; F, light green; S, yellow. The crystal structure was refined using NoSpherA2.^{37,38}

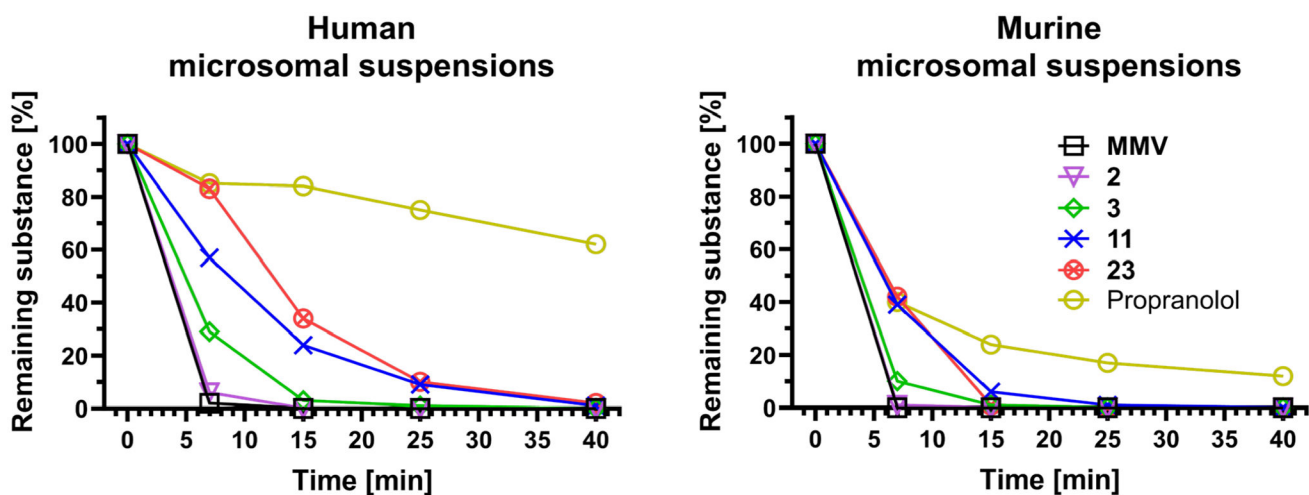


Figure 2. Degradation of a selection of compounds in human and murine microsomal suspensions over 40 min. Compounds **11** and **23** are shielded at aromatic system B with a 6-fluoro or 6-methyl substituent respectively and show higher stability than the unshielded derivatives (**3**). Displayed values are means of two replicates. Propranolol is shown as reference.

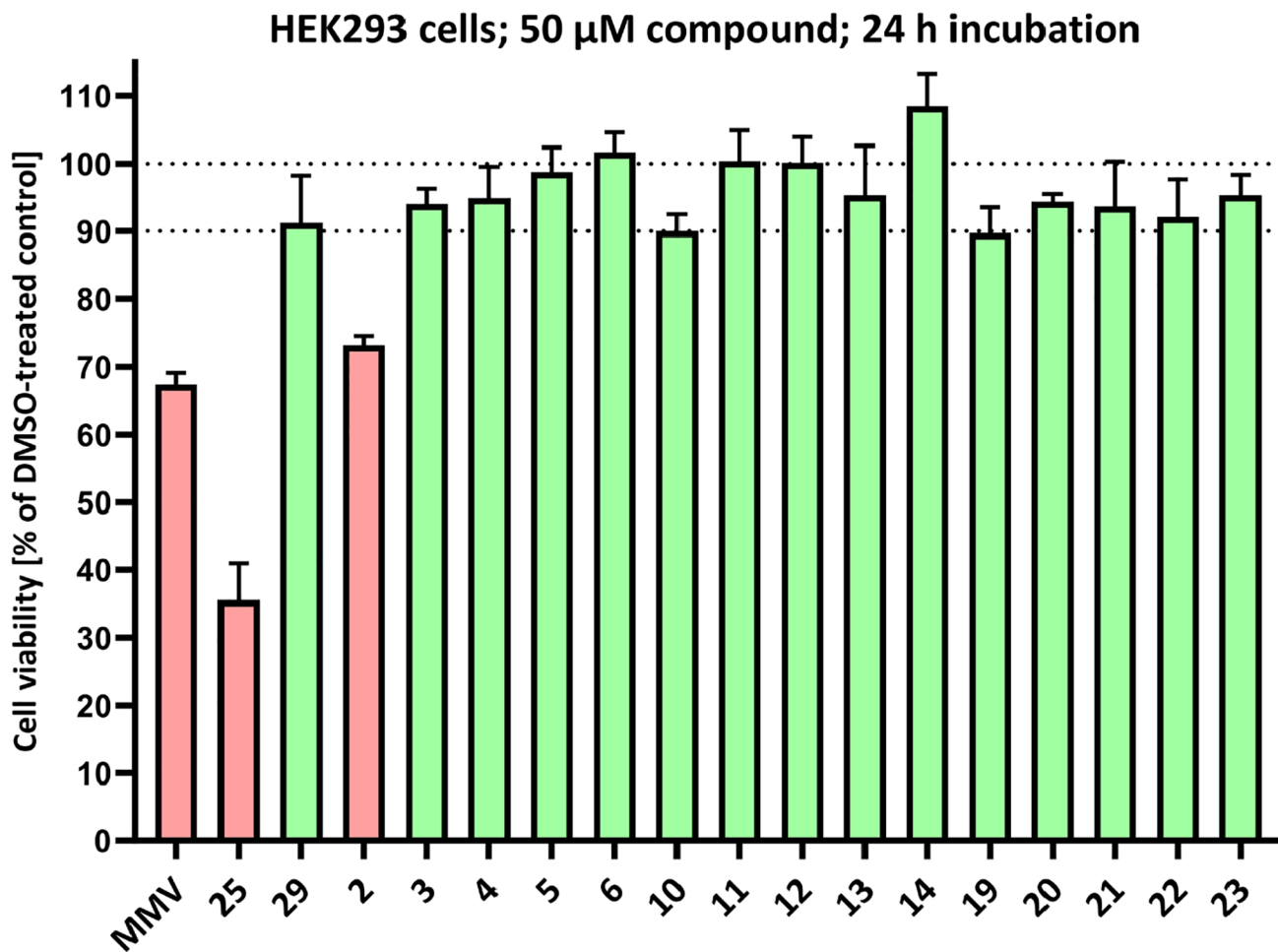
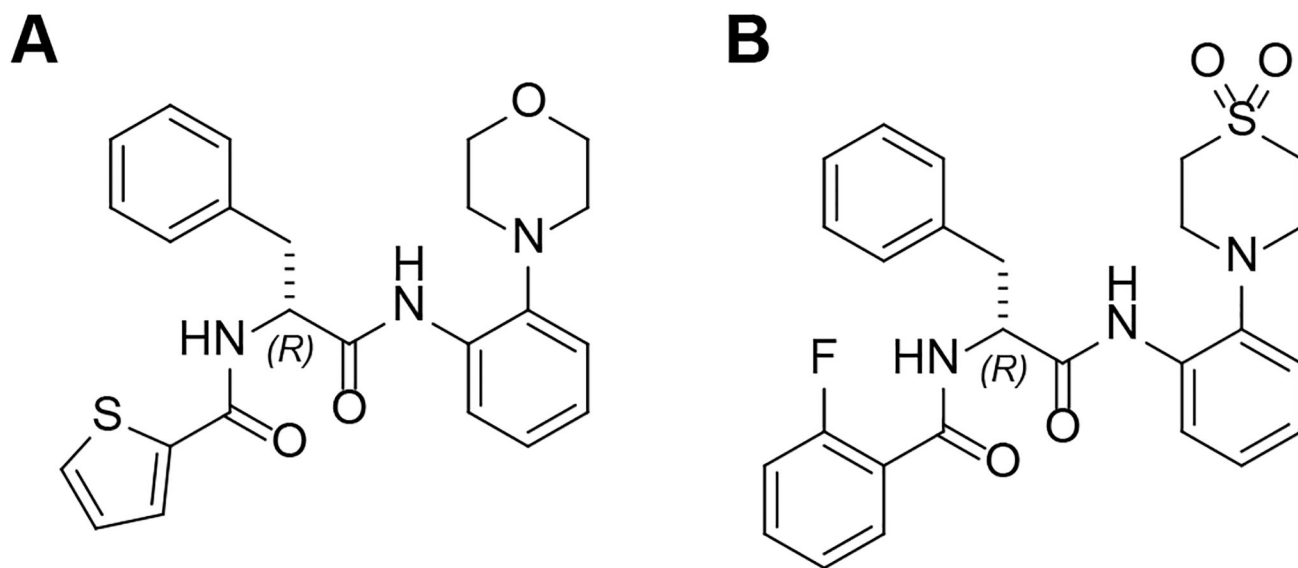
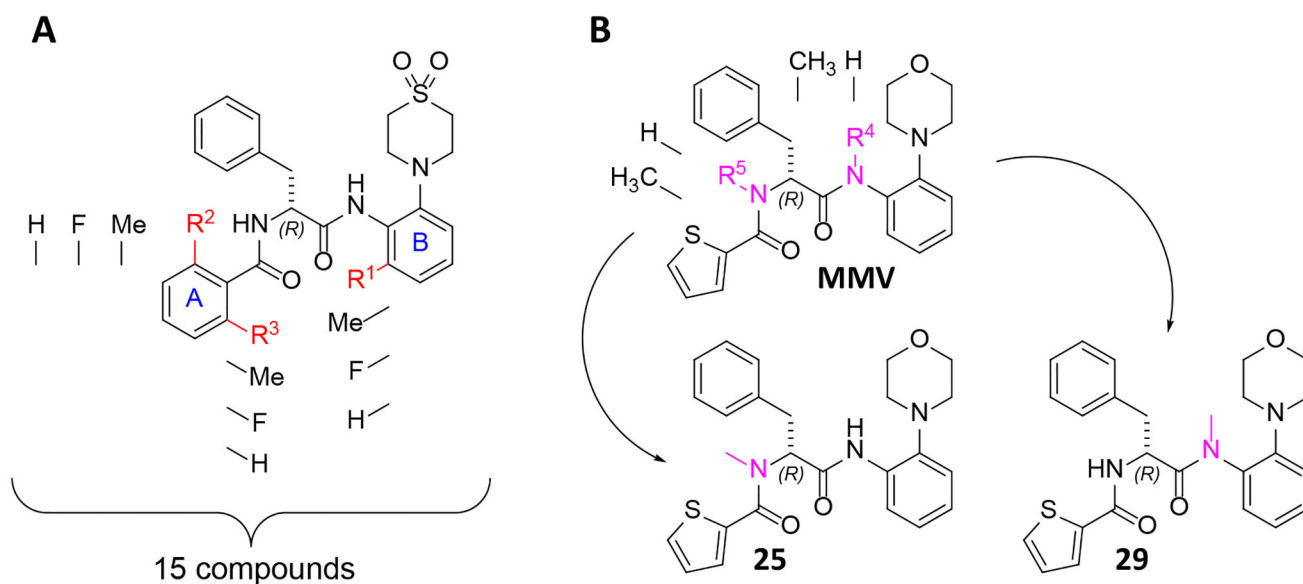


Figure 3. Cytotoxicity against human kidney epithelia cells HEK293. Determination of cell viability was performed at a single compound concentration of 50 μ M after 24 h of incubation relative to DMSO-treated cells. The displayed values are means \pm SD of triplicates. For detailed information of the protocol, see the Supporting information



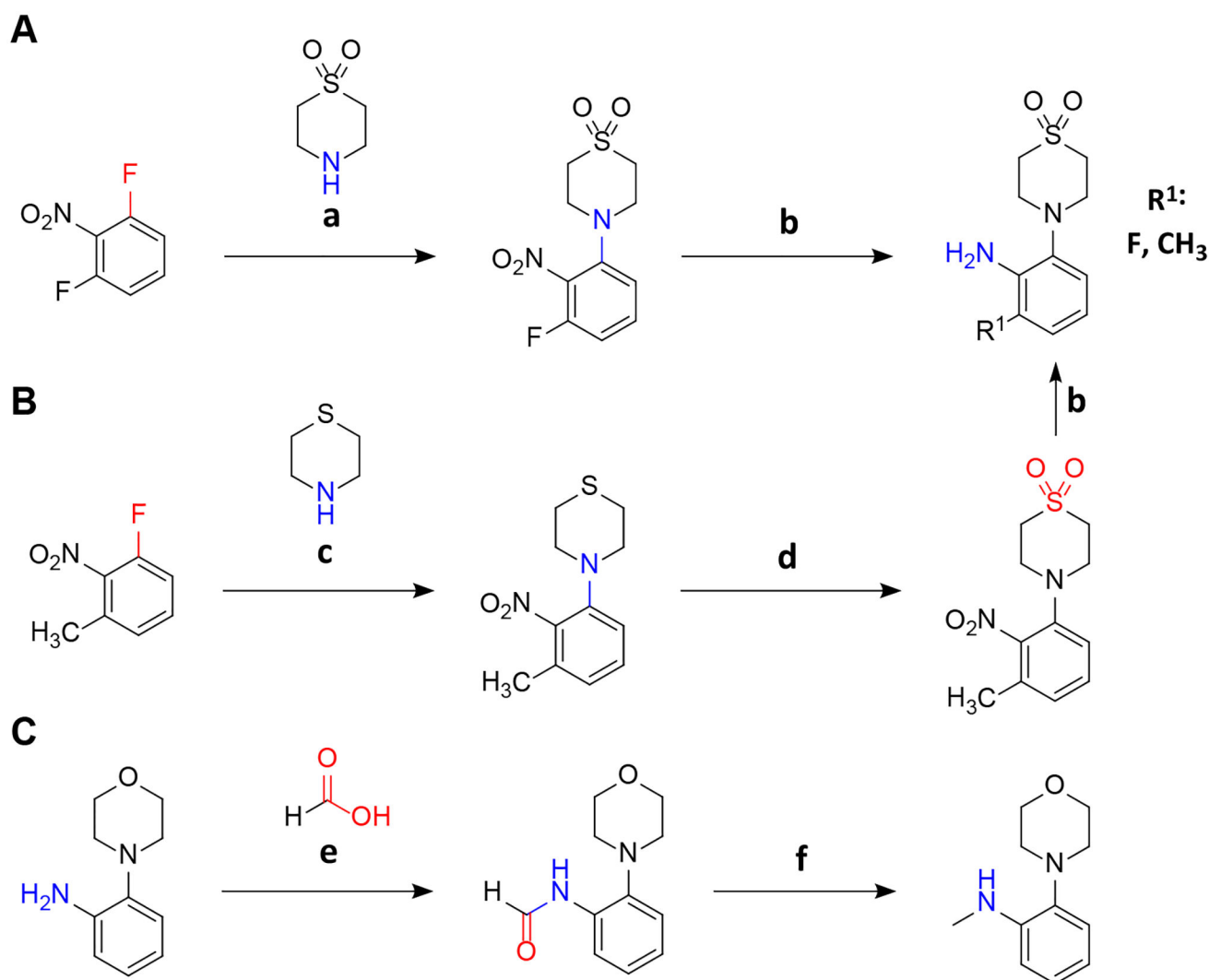
Scheme 1.

A: Molecular structure of the hit compound **MMV**. **B:** Molecular structure of **2**.



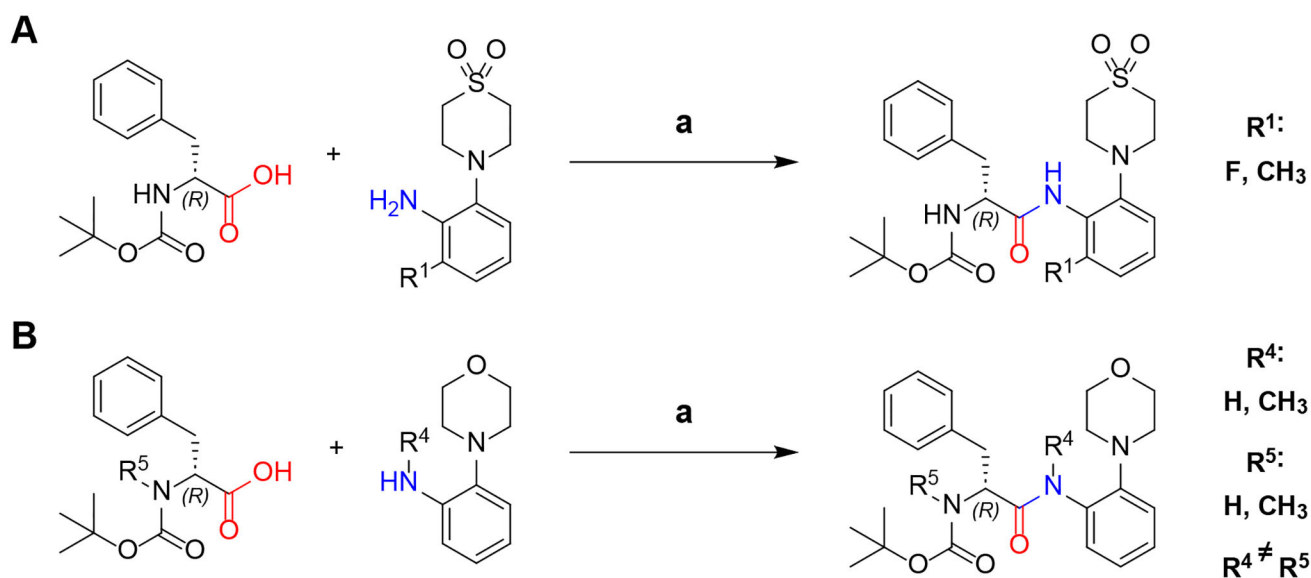
Scheme 2.

Derivatization strategy of AAPs for increased metabolic stability. **A:** The scaffold of (2*R*)-2-[(2-fluorophenyl)formamido]-*N*-[2-(1,1-dioxo-1λ6-thiomorpholin-4-yl)phenyl]-3-phenylpropanamide is depicted, and the changes at R^1 , R^2 , and R^3 are indicated. The synthesized derivatives contain either hydrogen, fluoro, or methyl substituents at the respective positions. All conceivable combinations within this range of substituents were synthesized, resulting in a total of 15 compounds. **B:** Two derivatives of **MMV** were synthesized by *N*-methylation at positions R^4 and R^5 . One compound was methylated at R^4 (**29**) and the other one at R^5 (**25**).

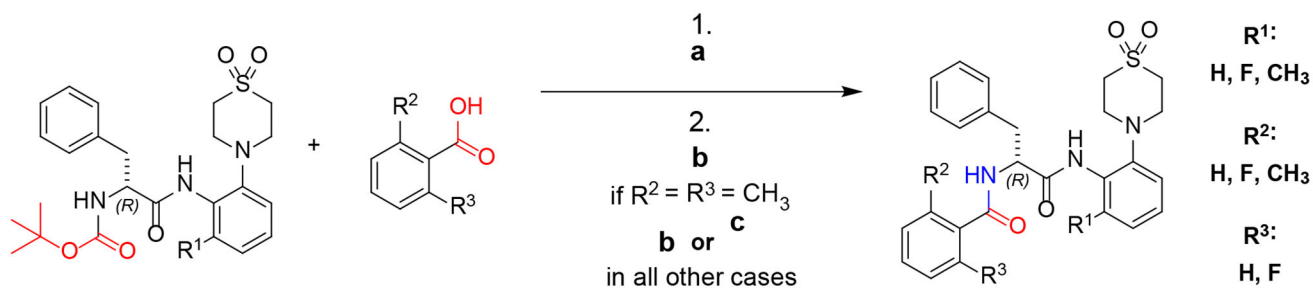
**Scheme 3.**

Synthesis of 4-(2-aminophenyl)-1 λ^6 -thiomorpholine-1,1-diones and *N*-methyl derivatives.

A: Synthesis of 3-fluoro derivatives. **B:** Synthesis of 3-methyl derivatives. **C:** Synthesis of *N*-methyl derivatives. **a:** DIPEA, 3 d, 50 °C; **b:** EtOH, H₂, Pd(OH)₂/C 20 %; **c:** DIPEA, 50 °C, 24 h; **d:** DCM, -20 °C, mCPBA in DCM added over 30 min; **e:** HCOOH, HCOONa, room temperature, overnight; **f:** THF, LiAlH₄ 1 M in THF dropwise over 30 min, argon, 0 °C to room temperature. For quantities and detailed procedures see Supporting Information.

**Scheme 4.**

Synthesis of *N*-Boc-(*R*)-phenylalanine anilides (**A**) and *N*-Boc-*N*-methyl-(*R*)-phenylalanine anilides (**B**). **a**: EtOAc + pyridine 2:1, T3P 50 % m/v in EtOAc, -20 °C to RT, 20 h. For quantities and detailed procedures see Supporting Information.

**Scheme 5.**

Synthesis of *N*α-2-phenoyl-(*R*)-phenylalanine-2-anilides. **a**: TFA, DCM, 1 h, RT; **b**: DMF, PyBOP, overnight, RT; **c**: Dioxane, DEPBT, overnight, RT. For synthesis of *N*-methyl compounds methods **a** and **b** were utilized (not depicted). For quantities and detailed procedures see Supporting Information.

Table 2.

Remaining substance [%] of AAP derivatives in murine and human microsomal suspensions after 7 min of incubation. Color coding compares remaining substance in the human and murine assays. Colors show the difference with respect to the average value. Dark green: highest percentage; light green: over average; white: closest to average; light red: below average, dark red: lowest percentage. The displayed values are means of two biological replicates. Propranolol was included as a reference.

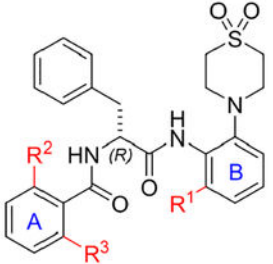
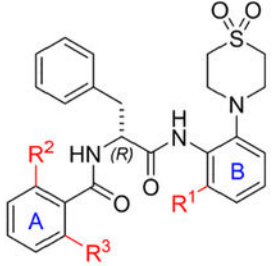
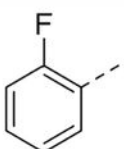
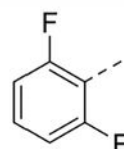
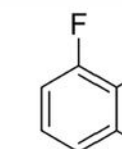
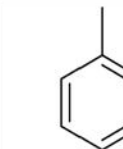
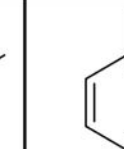
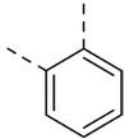
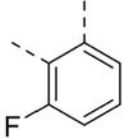
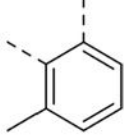
										Legend	
Core structure		MMV		25		29		Propranolol (control)		Substance Name	
		2	0	9	4	14	0	85	40	Human after 7 min [%]	Murine after 7 min [%]
		Aromatic system A									
Aromatic system B											

Table 3.

MIC₉₀ values of the new AAP derivatives against different mycobacteria. *Mabs* = *Mycobacterium abscessus* ATCC 19977; *Mintra* = *Mycobacterium intracellulare* ATCC 35761; *Mtb* = *Mycobacterium tuberculosis* H37Rv; *Mavium* = *Mycobacterium avium ssp. hominissuis* strain 109 (MAC109). Incubation at 37 °C for three days (*Mabs*), five days (*Mintra*) and seven days (*Mtb*). Experiments were performed in duplicate, results were averaged. Protocols for different strains differ slightly, for detailed information on the methodology see Supporting Information.

Core structure		MMV		25		29		Legend			
		6.25	0.78	100	> 100	100	> 100	Substance Name			
		0.66	3.02	> 50	> 50	> 50	> 50	<i>Mabs</i>	<i>Mintra</i>		
				> 50	> 50	> 50	> 50	<i>Mtb</i>	<i>Mavium</i>		
		Aromatic system A									
											
Aromatic system B		2		3		4		5		6	
		0.78	0.05	0.78	0.025	3.13	0.1	1.56	0.4	25	1.56
		0.25	0.99	0.15	0.6	0.66	1.47	0.4	1	13	10.4
		10		11		12		13		14	
		25	1.56	12.5	0.4	25	1.56	12.5	0.8	> 100	50
		16	12.9	5.5	5.43	28	13.5	12	9.8	13	> 50
	19		20		21		22		23		
	> 100	> 100	> 100	50	> 100	> 100	> 100	> 100	> 100	> 100	
	> 50	> 50	> 50	> 50	> 50	> 50	> 50	> 50	> 50	> 50	